ICSV 21
13-17 July, 2014, Beijing/China

The 21st International Congress on Sound and Vibration

13-17 July, 2014, Beijing/China

DEVELOPMENT OF A NUMERICAL MODEL FOR OBTAINING FLAME TRANSFER FUNCTION IN A SIMPLIFIED SLIT BURNER WITH HEAT EXCHANGER

Naseh Hosseini[1,2], Viktor Kornilov[1], O.J. Teerling[2], Ines Lopez Arteaga[1,3] and Philip de Goey[1]

1:Mechanical Engineering Department, Eindhoven University of Technology, Eindhoven, the Netherlands.
2:Bekaert Combustion Technology BV, Assen, the Netherlands.
3: Department of Aeronautical and Vehicle Engineering, KTH Royal Institute of Technology, Stockholm, Sweden

e-mail: n.hosseini@tue.nl

The goal of the present work is to develop a model to investigate the interactions between a burner and a heat exchanger, looking from a hydrodynamic and thermo-acoustic point of view. Thermo-acoustics of laminar premixed flames in open air have been studied by several researchers in the past decades. However, a burner in open air may behave differently compared to if situated in a combustion chamber enclosure. This could be related to the effect of temperature, the effect of flame shape (e.g. flames impinging on the heat exchanger walls in compact boilers), distribution of the flame on the burner deck, etc. The behavior of a linear array of a multiple Bunsen-type flames is studied on a 2D geometry in a CFD code to simulate the effects of heat exchanger addition on the thermo-acoustics of the flames. The location of the heat exchanger surface is varied for different conditions of power. A step profile velocity perturbation is used for obtaining the response of the flame represented within the flame transfer function approach. The calculated gain and phase of the flame transfer function are compared for different cases as the indicator of the thermo-acoustic behavior. Results show that the main parameter having considerable influence is the burner load and flame shape. The setup to experimentally investigate these effects will be constructed in near future.

1. Introduction

Perforated-plate stabilized flames are typical in industrial and compact household burners. Multiple conical premixed flames in these systems interact with each other and the system. Generally, the power output varies in a range that the flow through the perforated deck can be considered laminar. Some researchers have recently investigated such systems numerically, analytically and experimentally. Most of these investigations have considered flame(s) in open environment and studied the effects of different external parameters, as well as flame-flame and flame-burner deck interactions. It has been shown that the interactions of the flame with external perturbations and its surroundings is what defines the combustion dynamics in such laminar premixed systems.[1,2]

Acoustic waves are one of the main external parameters interacting with laminar flames. The unsteady heat release generated by this perturbation adds to or absorbs energy from the acoustic field

when it is in- or counter- phase with the pressure oscillations. In the worst case, these oscillations can lead to enhanced vibration, reduced part life, flame blowoff or flashback, and even system failure. A detailed review of modelling acoustic wave interactions in premixed combustion is available.[3]

In recent studies experimental and numerical investigations were performed to reveal the flame response to acoustic oscillations in a multi-slit Bunsen burner.[2] A transfer function was obtained and a transfer matrix was derived based on the Rankine-Hugoniot jump conditions. The study demonstrated that the numerical model was capable to reproduce all aspects observed in the experiments through a parametric study, where the mean flow velocity, the equivalence ratio, the slit width and the distance between slits are varied. The measured and computed flame transfer function were in good agreement.

Some researchers examined the impact of the operating conditions and the perforated-plate design on the steady, lean premixed flame characteristics.[4] They performed two-dimensional simulations of laminar flames using a reduced chemical kinetics mechanism for methane-air combustion. They suggested that the flame consumption speed, the flame structure, and the flame surface area depend significantly on the equivalence ratio, mean inlet velocity, the distance between the perforated-plate holes and the plate thermal conductivity. Other simulations of planar perforated-plate stabilized flames used solving the uncoupled 1-D unsteady conservation equations while using the G-equation to describe the flame motion and revealed similar results.[5,6]

The discussed models successfully predict the response of perforated-plate stabilized flames to acoustic waves as well as oscillatory heat loss to the burner surface. However, they are limited to laboratory flames in open environment, which is far from actual industrial applications. The mainly cost-driven motivation to make condensing boilers as compact as possible stimulates decrease of the distance between burner and heat exchanger. Combustion instabilities and thermoacoustics in such systems are among major concerns.

In general, a burner in open air behaves differently compared to if situated in a combustion chamber enclosure with flame-heat exchanger distance being small enough. This could be related to the effect of temperature, the effect of flame shape (e.g. flames impinging on the heat exchanger walls), distribution of the flame on the burner deck, etc.[7] In addition, it is not well known how to approach the problem to take into account the presence of a surface downstream of the flame, i.e. could it be treated as an oscillating heat sink and cause additional acoustic source in the whole system.

The general goal of the present work is to reveal the physics of the interactions between a burner and a heat exchanger looking from a hydrodynamic and thermo-acoustic point of view. One approach to this problem is by means of using CFD to simulate the thermo-acoustic effects of heat exchanger addition in a linear array of a multiple Bunsen-type flames. The system under investigation is a flat multi-slit burner with the geometry shown in Fig. 1. Within the present contribution the method of modelling, implementation of CFD setup, validation of the simulations and first illustrative results will be discussed.

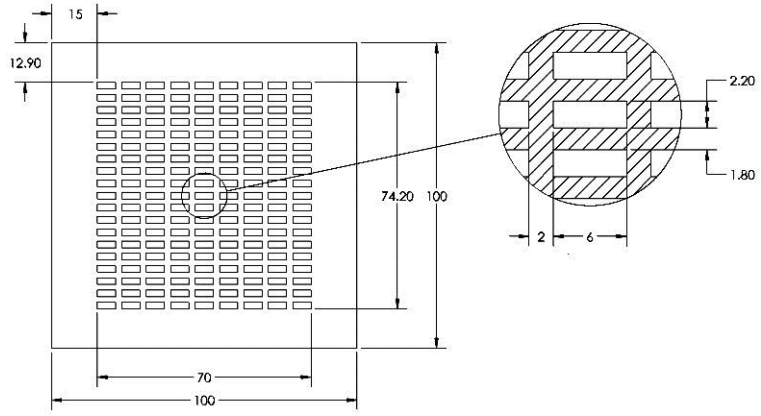

Figure 1. Burner deck (all dimensions in millimetres).

2. Numerical model

In order to model this geometry, a 2D domain has been generated in Gambit, which corresponds to one slit in the burner. Symmetry has been used on both sides to include the effects of neighboring flames as well as reducing the domain size. Figure 2 shows the dimensions (in millimeters) and the boundary conditions of the domain.

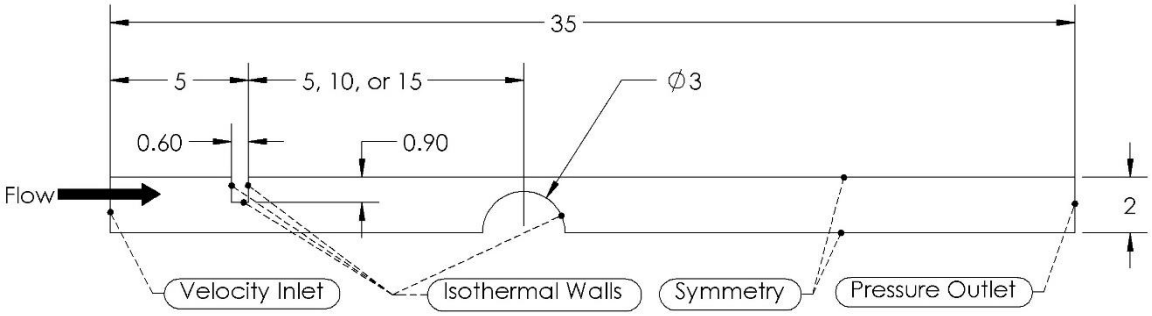

Figure 2. Numerical domain and boundary conditions.

2.1 Assumptions and equations

The flow in the domain has been considered laminar due to low Reynolds numbers. The burner deck and heat exchanger surface have been assumed to be at constant temperatures of 500 and 350K, respectively. Methane-air mixture enters the system with equivalence ratio of 0.8 after complete mixing has been achieved. Finite rate chemistry combustion model has been used to model gas phase combustion in the domain. The outlet boundary condition has been fixed at atmospheric pressure.

The commercial CFD code, ANSYS Fluent, has been used for the numerical calculations. The local mass fraction of each species Y_i is predicted through the solution of a convection-diffusion equation for the i^{th} species. This conservation equation takes the following general form:

$$\frac{\partial}{\partial t}\left(\rho Y_i\right)+\nabla.\left(\rho\vec{v}Y_i\right)=-\nabla.\vec{J_i}+R_i+S_i \tag{1}$$

where R_i is the net rate of production of species i by chemical reaction and S_i is the rate of creation by addition from the dispersed phase plus any user-defined sources. An equation of this form will be solved for $N-1$ species where N is the total number of fluid phase chemical species present in the system. Since the mass fraction of the species must sum to unity, the N^{th} mass fraction is determined as one minus the sum of the $N-1$ solved mass fractions.[8]

The reaction at lean conditions can be written in the following global form:

$$CH_4+2\left(O_2+3.76N_2\right)\rightarrow CO_2+2H_2O+7.52N_2 \tag{2}$$

The rate constant for the reaction, k_r, is computed using the Arrhenius expression as:[8]

$$k_r=A_rT^{\beta_r}e^{-E_r/RT} \tag{3}$$

where,

A_r = pre-exponential factor (consistent units), which has been set to 2.29×10^{19}

β_r = temperature exponent (dimensionless), which was set to 2.8 and 1.2 for CH_4 and O_2, respectively

E_r = activation energy for the reaction (J/kmol), which has been set to 1.38×10^{8} in Fluent database

R = universal gas constant (J/kmol-K), which is set to 8314.34 in Fluent database

The mentioned pre-exponential factor and the rate exponent values have been modified from default values in Fluent in order to achieve better agreement in laminar burning velocity with the data available in the literature. The results of these modifications are presented in the next section.

2.2 Verifications

In order to find the optimum spatial and temporal resolution, pseudo-1D simulations have been performed in a domain with negligible height with respect to length (0.02×35mm) to verify the laminar burning velocity (S_b) sensitivity to grid size, equivalence ratio an unburnt mixture temperature. Results show that a time step of 0.01ms with the grid size of 0.02mm is required to accurately capture the chemistry. Figure 3 shows the results for grid dependency test.

Gambit has been used to generate a 2D mesh for numerical calculations using the verified 1D grid size. The generated mesh is illustrated at three different zoom levels in Fig. 4. Because the heat exchanger surface will be present at different distances, the mesh cannot be coarsened downstream of the flame. The final mesh comprises 164689 elements.

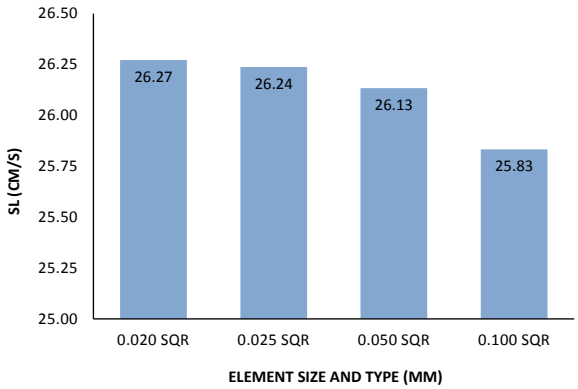

Figure 3. Grid dependency analysis.

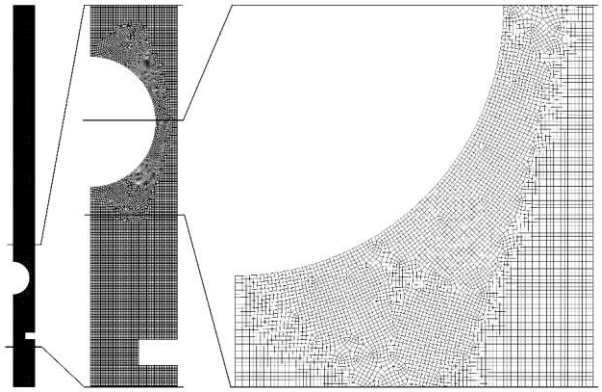

Figure 4. 2D numerical grid.

The equivalence ratio and unburnt temperature sensitivity analysis results are presented in Figs 5 and 6. Good agreement between the 1D model and the literature can be observed.

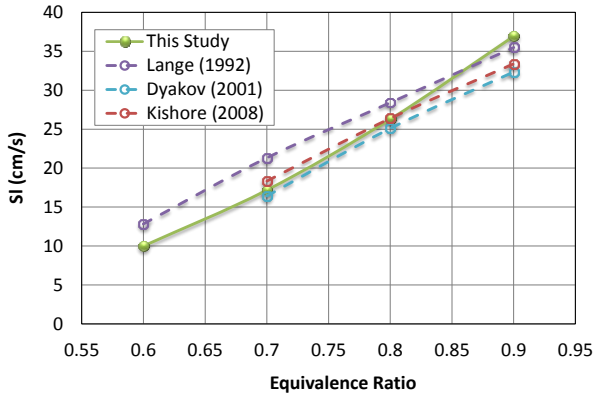

Figure 5. Equivalence ratio sensitivity analysis.

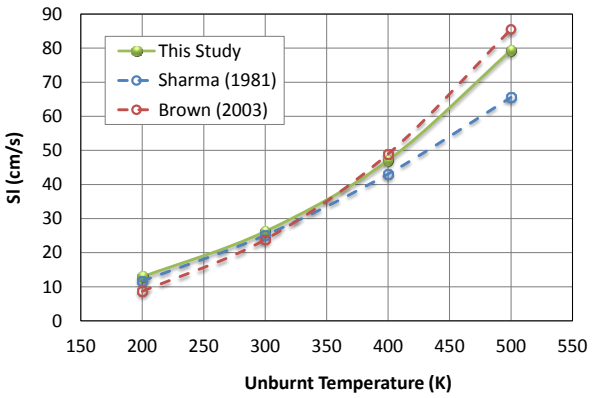

Figure 6. Unburnt temperature sensitivity analysis.

2.3 Transfer function

The flame transfer function can be used for system instability prediction. Via a transfer function, the relation between the input and output is described.[9,10] In this study, the flame transfer function is calculated via a velocity perturbation as the input and heat release rate as the output. For premixed flames in a limited range of perturbations, it is assumed that the flame response scales linearly with the upstream perturbation.[11] The (complex) flame transfer function is defined as:

$$TF(f) = \frac{q'(f)/\bar{q}}{u'(f)/\bar{u}} \tag{4}$$

where $q'(f)$ is the oscillating heat release rate, $u'(f)$ is the upstream velocity perturbation, $\bar{q}$ is the mean heat release rate, $\bar{u}$ is the mean velocity and f is the frequency. $\bar{q}$ and $\bar{u}$ are introduced for normalization. Thus, the transfer function is the relative flame response divided by the relative upstream velocity perturbation.[11]

2.4 Case studies

In this study a step profile with 5% increase was used for inlet velocity perturbations. A step profile is numerically easy to produce and also includes every frequency. Thus, with a single excitation the whole frequency domain response can be covered, assuming that response is in the linear regime. After each increase there is 40 milliseconds relaxation time. The inverse step is then manually calculated to generate a periodic signal for Fourier transformation in transfer function calculations. The two main parameters under investigation have been burner load and the distance between the heat exchanger and the burner deck. Table 1 summarizes the configurations of the case studies.

Table 1. Case studies configurations.

		Heat exchanger-burner deck Distance (mm)			
		N/A	5	10	15
Inlet Velocity (cm/s)	25	NoHex-V25	Hex05-V25	Hex10-V25	Hex15-V25
	50	NoHex-V50	Hex05-V50	Hex10-V50	Hex15-V50

3. Results and discussion

The simulations have been performed for the 8 cases mentioned in Table. 1. It is worth mentioning that the calculations have been considerably intensive, in the order of 10-20 hours on a Linux machine with two 8-core AMD Opteron 2.4 GHz CPUs.

Figures 7 and 8 show a comparison of the temperature and reaction rate in all the cases. For every pair of contours the left and right one correspond to low and high burner loads, respectively. It can be observed that the case with high load and low distance between flame and heat exchanger (Hex05-V50) is the most deviating case. This is due to intense flame cooling and also changes in flame shape that can considerably affect the flame behaviour and transfer function. [1,2,7] It can also be observed that higher loads lead to higher post flame temperatures.

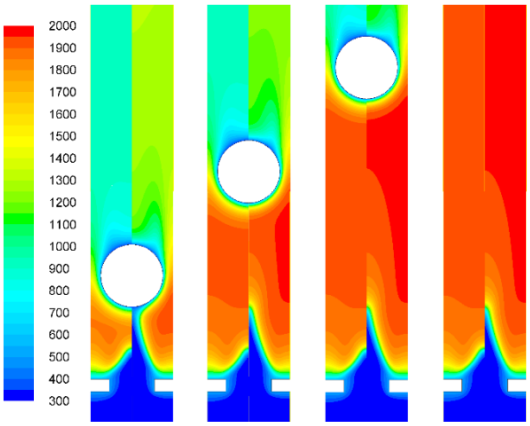

Figure 7. Temperature (K), left: V=25cm/s, right: V=50cm/s.

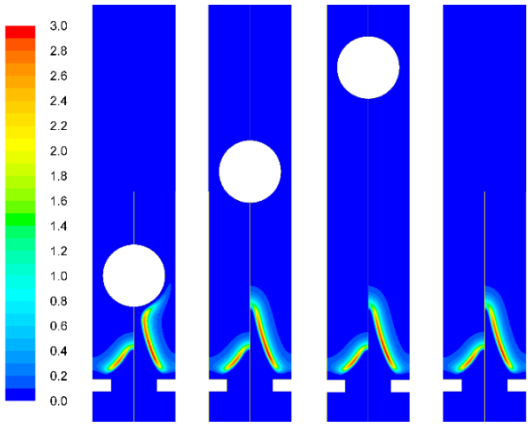

Figure 8. Reaction rate (kmol/m^{3}s), left: V=25cm/s, right: V=50cm/s.

Details of the flow field and flame shape in the most deviating case is represented via velocity vectors and the reaction rate contour for two zoom levels in Fig. 9. The deviation of the flow due to the presence of the heat exchanger surface and also acceleration through the flame front is visible in this figure. In addition, the wake behind the cylinder has been captured properly.

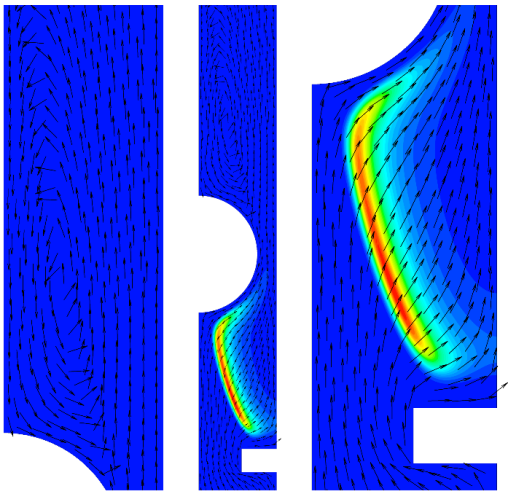

Figure 9. Velocity vectors and reaction rate contour.

The flow velocity has been monitored at different locations on the flame axis. The location corresponding to the bottom side of the burner deck has been chosen for calculation of the transfer function due to better compatibility to the future experiments. The sum of heat release rate in the domain and the heat flux through heat exchanger and burner deck surfaces have been monitored during calculations.

The flame transfer function has been calculated for all the cases considering the selected location velocity as excitation and the total reaction heat release rate as response. The variations of the excitation and response signals as function of time for the high load cases are plotted in Fig. 10. The excitation takes place at 120ms and it can be seen that the ideal step profile at the inlet changes to a smoother profile before the burner deck due to area change and flow straining. The heat release rate decreases as the heat exchanger approaches the burner deck, which has been expected due to increased flame cooling.

Figure 11 shows another representation of the heat release rate time series. In this figure, all the values have been normalized with respect to their corresponding values before excitation. Moreover, time has been shifted to zero for convenience. It can be observed that all cases behave similarly, except the most deviating case with flame impingement. The peak value for the relative heat release rate in this case is lower and also happens around 1ms later compared to the other cases. In addition, the normalized values for all the cases converge to 1.05, which corresponds to the excitation amplitude. But for the impinging case reaches a value of 1.053, which can be a sign of some degree of offset in the system that needs to be investigated further.

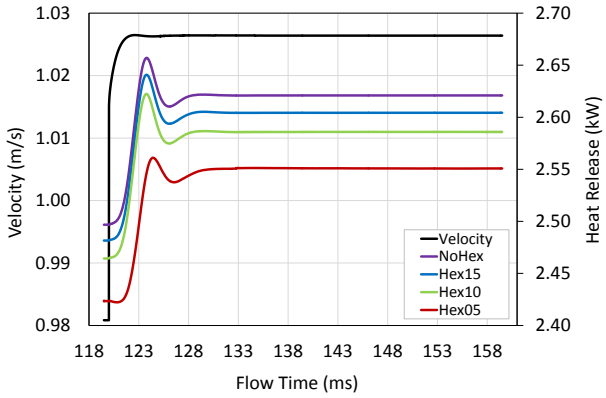

Figure 10. Velocity excitation at the burner deck and heat release rate time series for V=50cm/s.

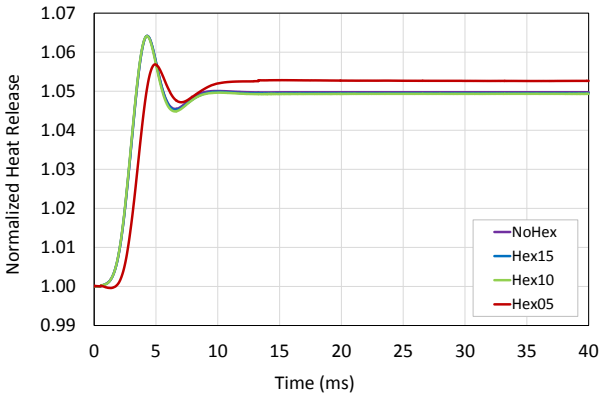

Figure 11. Normalized heat release rate time series for V=50cm/s.

The time series data has been transformed into frequency domain using Fourier transformation and the complex transfer function has been calculated. The transfer function gain and phase are plotted in Figs. 12 to 15. Figures 12 and 13 correspond to low burner load (inlet velocity 25 cm/s), while Figs. 14 and 15 correspond to high burner load (inlet velocity 50cm/s). The range of the figures have been adjusted accordingly. It can be seen that the gain and phase of the transfer function does not considerably change when the flame is not deformed by the heat exchanger surface.

For all the cases there is no considerable gain value for frequencies above 500 Hz. Some fluctuations for frequencies higher than 500Hz have been greyed out. This is because the gain for this high frequencies is almost zero and in this range it can cause numerical errors in the phase by dividing two very small values. Thus, this part of the data cannot be interpreted.

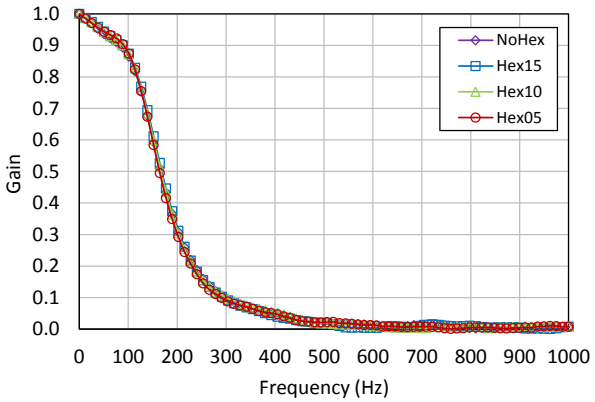

Figure 12. Transfer function gain for V=25cm/s.

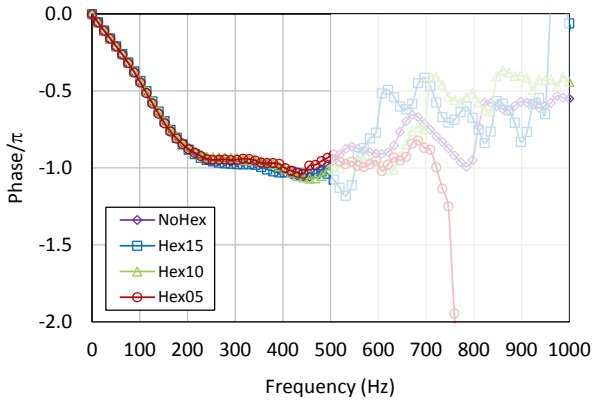

Figure 13. Transfer function phase for V=25cm/s.

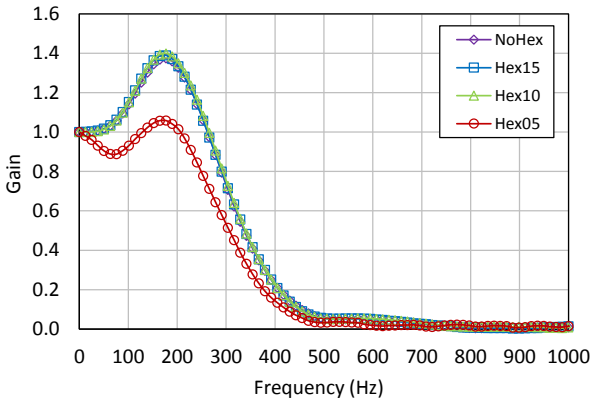

Figure 14. Transfer function gain for V=50cm/s.

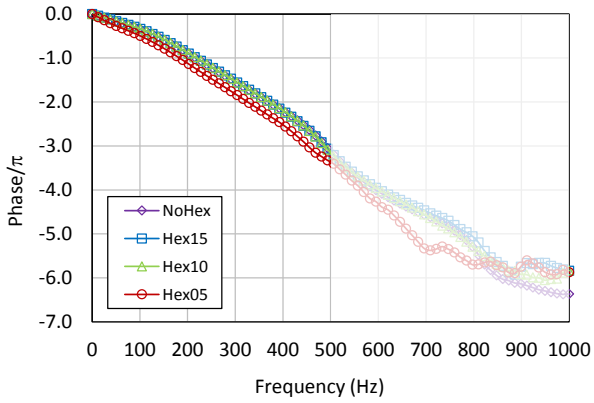

Figure 15. Transfer function phase for V=50cm/s.

For all low load cases the gain has its maximum value at zero frequency and its variations with frequency does not change as the heat exchanger moves towards the flame. This is due to the fact that the flame does not impinge on the heat exchanger surface, even for the case with minimum distance between the burner deck and heat exchanger. However, the gain in high load cases overshoots unity at some frequency below 200Hz. The gain for the impinging case is lower than the other cases and has a negative slope at zero frequency.

For the high load cases the phase diagram crosses -2π at 370Hz for the non-impinging cases and at 330Hz for the impinging case, which shows more than 10% difference in the frequency, corresponding to some difference in the time delay between these cases. Generally, time delay for all the case studies has a similar value.

4. Conclusions

A CFD model was developed to study the transfer function of a slit burner with heat exchanger. The model uses a modified single-step chemistry in laminar flow to predict the flow field, combustion, and the response of the flame to velocity oscillations. The model was investigated to accurately simulate the flame speed and it demonstrated good agreement in sensitivity analysis. The model was then further developed to 2D to simulate a flame anchored on perforated plate. Different cases with and without heat exchanger were studied. It was shown that the presence of the heat exchanger surface for distances that do not cause flame impingement, changes the absolute value of the heat release rate of the flame, but the normalized values and the transfer function of the flame stay the same. Flame impingement due to close distances between the burner deck and heat exchanger changes the flame shape. This changes the behaviour of heat release rate in a way that the transfer function is also affected. Some degree of offset was also seen for this case. The research on the transfer function for impinging flame cases is a work in progress and an experimental setup of the same dimensions is being constructed to further validate the 2D model in near future.

ACKNOWLEDGEMENT

The presented work is part of the Marie Curie Initial Training Network Thermo-acoustic and aero-acoustic nonlinearities in green combustors with orifice structures (TANGO). We gratefully acknowledge the financial support from the European Commission under call FP7-PEOPLE-ITN-2012.

REFERENCES

[1] Altay, H.M., Park, S., Wu, D., Annaswamy, A.M. and Ghoniem, A.F. Modeling the Dynamic Response of a Laminar Perforated-plate Stabilized Flame, *Proceedings of the Combustion Institute*, **32**, 1359–1366, (2009).

[2] Kornilov, V.N., Rook, R., ten Thije Boonkkamp, J.H.M. and de Goey, L.P.H. Experimental and Numerical Investigation of the Acoustic Response of Multi-slit Bunsen Burners, *Combustion and Flame*, **156**, 1957–1970, (2009).

[3] Lieuwen, T. Modeling Premixed Combustion–Acoustic Wave Interactions: A Review, *Journal of Propulsion and Power*, **19** (5), 765–781, (2003).

[4] Altay, H.M. , Kedia, K.S. , Speth, R.L. and Ghoniem, A.F. Two-dimensional Simulations of Steady Perforated-plate Stabilized Premixed Flames, *Combustion Theory and Modelling*, **14** (1), 125–154, (2010).

[5] Rook, R., de Goey, L.P.H., Somers, L.M.T., Schreel, K.R.A.M. and Parchen, R. Response of Burner-stabilized Flat Flames to Acoustic Perturbations, *Combustion Theory and Modelling*, **6**, 223–242, (2002).

[6] Schreel, K.R.A.M., Rook, R. and de Goey, L.P.H., The Acoustic Response of Burner-stabilized Premixed Flat Flames, *Proceedings of the Combustion Institute*, **29**, 115–122, (2002).

[7] Fernandes, E.C. and Leandro, R.E. Modeling and Experimental Validation of Unsteady Impinging Flames, *Combustion and Flame*, **146**, 674–686, (2006).

[8] ANSYS, Inc., *ANSYS FLUENT Theory Guide*, SAS IP Inc., Canonsburg, PA, 177–181, (2012).

[9] Manohar, *Thermo-acoustics of Bunsen Type Premixed Flames*, Doctor of Philosophy Thesis, Graduate Program in Mechanical Engineering, Eindhoven University of Technology, (2011).

[10] Looijmans, J.M.M., *Thermoacoustic Stability of Combustion in Central Heating Boilers*, Master of Science Thesis, Graduate Program in Mechanical Engineering, Eindhoven University of Technology, (2010).

[11] Kornilov, V., *Experimental Research of Acoustically Perturbed Bunsen Flames*, Doctor of Philosophy Thesis, Graduate Program in Mechanical Engineering, Eindhoven University of Technology, (2006).